ELSEVIER

Physics of the Earth and Planetary Interiors 87 (1995) 183–196

PHYSICS
OF THE EARTH
AND PLANETARY
INTERIORS

Anisotropy of magnetic susceptibility in the Ponta Grossa dyke swarm (Brazil) and its relationship with magma flow direction

Maria Irene Bartolomeu Raposo *, Marcia Ernesto

Instituto Astronômico e Geofísico, University of São Paulo, C.P. 9638, 01065-970 São Paulo, Brazil

Received 13 July 1993; revision accepted 24 June 1994

Abstract

Measurements of anisotropy of magnetic susceptibility (AMS) in 95 mafic dykes (mainly tholeiites 10–200 m in width) from the Mesozoic Ponta Grossa swarm, Southern Brazil, revealed two main types of magnetic fabric. Type I fabric (plane K_1–K_2 parallel to the dyke plane) represents magma flow within the dykes, whereas Type II (plane K_1–K_3 parallel to the dyke plane) is compatible with a fabric pattern reflecting vertical compaction of the magma column. Fabric Type I dominates (51% of the dykes) within the swarm, whereas Type II (38% of the dykes) concentrates mainly in the western region where the dykes intrude sediments. Considering the dykes with Type I fabrics, it is concluded that 58% of the dykes were fed by horizontal or sub-horizontal (K_1 inclinations less than 30°) magmatic flow, and 42% were fed by inclined to vertical (K_1 inclinations more than 30°) magma flow. The latter are more frequent in the southeastern part of the swarm, suggesting a magma source close to this area, although there may have been other sources in other regions where dykes with inclined flow and distinct chemical characteristics are also found.

1. Introduction

In recent years there has been growing interest in the investigation of dyke emplacement processes, not only because dykes represent former conduits for the passage of magma from deeper levels of the Earth to the surface but also because dyke swarms give information about tectonic processes that deformed the lithosphere. The flow of magma inside fractures is one issue of basic importance in understanding how continental swarms developed. Magma flow directions are traditionally investigated by means of petrographic fabric (e.g. Komar, 1972; Shelley, 1985; Ross, 1986; Greenough et al., 1988), oriented vesicles (e.g. Coward, 1980) and fingers, grooves or lineations (e.g. Baer and Reches, 1987). However, these methods are not useful when the petrographic fabric is poorly defined. Even when the fabric is strongly developed, observations made on oriented thin sections under the microscope are tedious, and methods based on field observations of flow structures must be used with care, as a distinction between lineations and grooves is not always evident or these indicators are simply absent.

The anisotropy of magnetic susceptibility (AMS) has long been a useful tool to investigate problems in sedimentology, tectonics and igneous

* Corresponding author. e-mail: mernesto@fox.cce.usp.br.

SSDI 0031-9201(94)02970-9

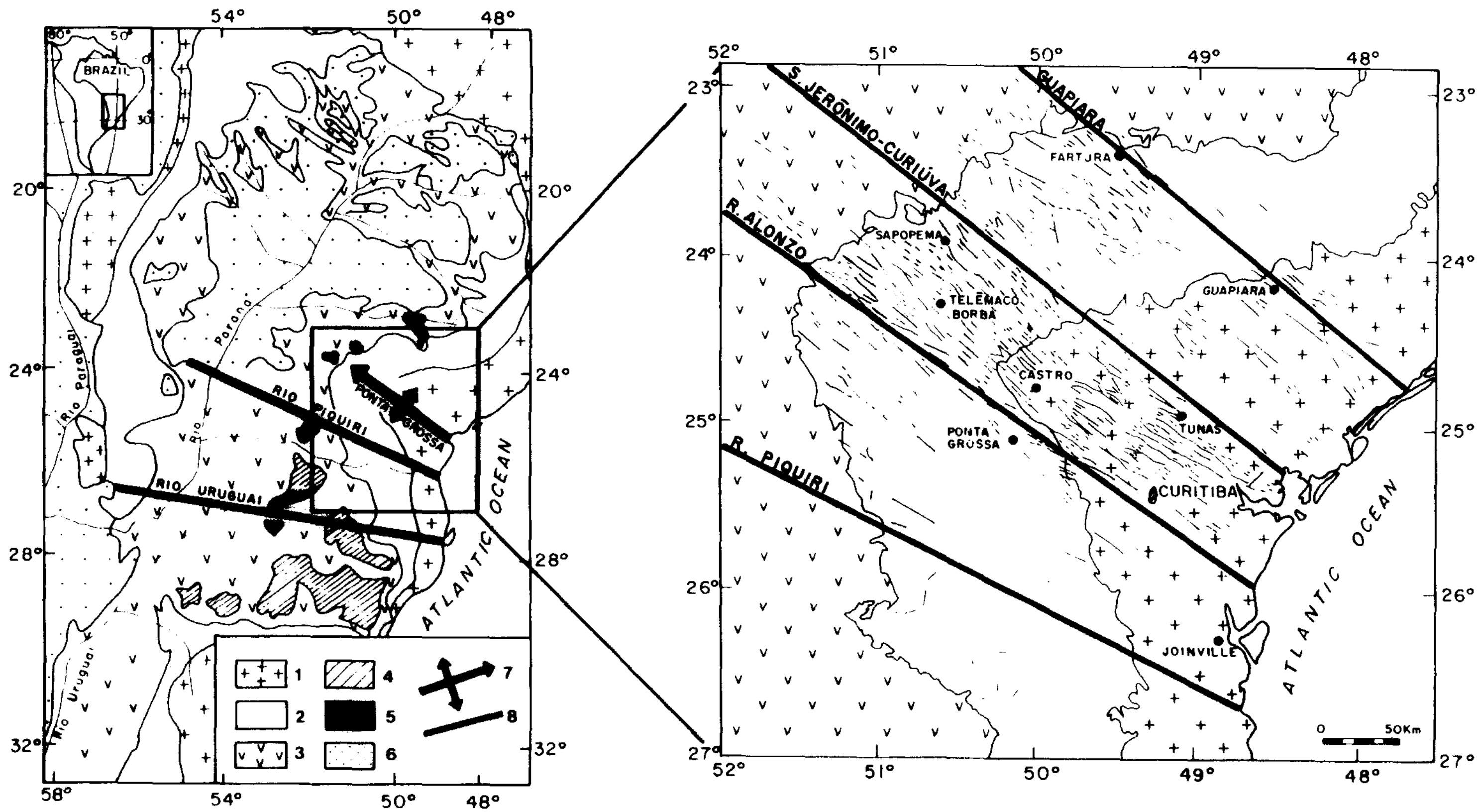

Fig. 1. Generalized geological map of the Paraná Basin showing the Ponta Grossa Arch: (1) crystalline basement; (2) pre-volcanic sediments (mainly Palaeozoic); (3) basic to intermediate flood volcanics from the Serra Geral Formation; (4) acid lava flows (Palmas type); (5) acid lava flows (Chapecó type); (6) post-volcanic sediments (mainly upper Cretaceous); (7) arch-type structure; (8) tectonic and/or magnetic lineaments.

Table 1
AMS data for the Ponta Grossa dykes

Site	N/n	K_1			K_2			K_3			K	P	L	F	Width	Strike	Fabric
		Decl.	Incl.	Ci	Decl.	Incl.	Ci	Decl.	Incl.	Ci	(10^{-3})	K_1/K_3	K_1/K_2	K_2/K_3	(m)		type
Fartura																	
1	5/ 5	287.8	40.3	48.8	350.5	4.5	48.3	53.2	0.1	50.5	28.136	1.0286	1.014	1.015	30	N41W	I
2	5/ 5	36.8	40.2	51.6	308.3	−3.3	50.9	36.2	−42.4	26.1	33.585	1.0191	1.007	1.012	?	N-S	IIb
3	4/ 4	310.4	−2.5	43.8	34.1	18.8	62.5	77.9	−88.6	45.9	28.748	1.0058	1.004	1.002	?	N36W	IIa
4	13/10	305.5	−4.1	17.2	26.7	65.2	46.3	39.2	−22.4	46.7	81.960	1.0130	1.010	1.003	?	N24W	I
6	12/12	286.2	18.3	35.8	335.0	−53.4	53.5	22.1	28.8	43.3	50.265	1.0100	1.006	1.003	40	N60W	I
7	3/ 3	32.4	−10.6	26.1	307.9	21.2	22.8	276.1	−68.8	29.1	3.782	1.0098	1.008	1.002	50	N4E	IIa
9	12/10	18.8	16.3	44.4	294.8	10.0	37.5	335.3	−74.6	43.6	34.080	1.0149	1.006	1.008	?	N34E	IIa
10	22/22	–	–	–	–	–	–	–	–	–	38.239	1.0159	1.008	1.007	30	N26W	IV
18	6/ 6	59.7	1.7	50.2	330.0	−5.9	50.3	314.5	82.6	9.5	21.503	1.0314	1.008	1.023	?	N87E	IIa
19	11/11	336.9	−3.2	59.5	60.3	11.8	39.0	88.7	−54.4	59.2	26.578	1.0090	1.004	1.005	10	N54W	IIa
21	14/14	–	–	–	–	–	–	–	–	–	54.928	1.0070	1.003	1.004	100	N86W	IV
22	8/ 7	293.7	−12.9	28.1	89.2	−70.0	38.9	19.6	7.4	34.1	17.166	1.0096	1.006	1.004	15	N65W	I
23	8/ 7	61.1	18.3	27.6	342.2	−24.1	20.4	299.6	57.5	27.3	33.437	1.0208	1.011	1.010	50	N76W	IIa
84	12/11	296.8	2.3	42.5	28.1	71.9	50.3	31.1	−21.2	35.8	31.039	1.0176	1.007	1.011	100	N76W	I
119	15/10	292.1	9.7	23.2	22.5	9.2	33.2	347.2	−77.5	28.9	38.738	1.0537	1.011	1.042	?	N51W	IIa
120	12/12	25.4	25.5	29.8	294.8	6.2	27.4	9.6	−63.6	20.8	32.867	1.0289	1.011	1.018	70	N30E	IIa
121	20/15	276.7	19.2	51.2	35.7	43.9	52.0	359.8	−23.3	51.6	36.355	1.0341	1.015	1.019	50	N60W	I
Sapopema																	
24	11/ 8	318.6	6.7	27.6	48.5	8.0	31.6	3.3	−77.9	18.6	45.052	1.0305	1.010	1.021	?	N51W	IIa
26	9/ 8	326.2	0.6	13.5	56.3	10.7	9.1	52.3	−79.7	12.4	36.202	1.0202	1.006	1.014	30	N25W	IIa
27	9/ 9	307.3	14.6	57.2	37.0	−8.3	52.8	278.5	−71.5	27.3	68.147	1.0444	1.011	1.033	100	N-S	IIa
28	18/18	66.2	0.5	53.6	337.6	−1.3	52.5	85.2	−87.7	16.7	44.736	1.0189	1.006	1.013	70	N65E	IIa
29	8/ 8	329.5	−55.7	29.3	304.1	32.8	29.5	40.6	11.7	14.7	53.791	1.0286	1.010	1.018	500	N45W	I
31	5/ 5	328.8	−77.4	16.0	291.6	7.1	34.8	22.4	8.2	34.1	66.331	1.0394	1.021	1.018	40	N30E	IIb
32	7/ 7	314.2	46.8	49.3	26.1	−3.7	43.6	276.1	−33.2	49.2	47.338	1.0156	1.004	1.011	?	N35W	IIb
33	8/ 6	345.8	−8.5	46.9	73.9	−12.0	54.6	78.1	79.3	28.7	56.436	1.0162	1.007	1.009	300	N60W	IIa
34	7/ 6	349.4	−4.8	38.7	82.1	10.3	53.0	326.3	84.3	41.8	41.764	1.0101	1.004	1.006	50	N35W	IIa
35	7/ 6	327.6	19.7	33.8	356.5	−59.4	52.0	68.9	17.6	54.6	52.670	1.0156	1.008	1.008	50	N20W	I
47	4/ 4	84.2	82.2	35.9	304.2	4.3	50.4	33.5	−7.5	35.2	34.615	1.0176	1.008	1.009	50	N45E	IIb
52	12/12	332.1	2.9	53.3	58.4	−21.4	54.5	271.7	−77.3	34.9	38.905	1.0255	1.010	1.016	?	N30W	IIa
Telêmaco Borba																	
36	12/12	357.8	86.5	43.3	280.7	11.3	56.1	12.6	−2.2	46.0	54.314	1.0233	1.015	1.008	20	N15W	IIb
37	8/ 8	274.2	−1.2	31.1	4.7	−7.4	32.9	357.8	82.9	13.6	49.268	1.0217	1.007	1.014	100	N80E	IIa
39	6/ 6	34.7	−11.2	54.7	293.3	75.6	61.6	294.2	−12.6	40.9	49.366	1.0142	1.003	1.011	30	N75E	I
41	4/ 4	279.6	13.8	15.1	52.8	70.0	28.9	3.1	−12.8	25.3	40.902	1.0111	1.006	1.005	?	N80W	I
42	4/ 4	84.5	3.2	37.8	354.7	−4.4	39.7	5.6	86.5	12.7	30.069	1.0342	1.011	1.023	50	N65W	IIa
44	9/ 9	313.0	5.0	16.8	45.9	14.1	36.1	27.1	−76.4	38.4	30.896	1.0276	1.021	1.007	30	N53W	IIa
45	4/ 4	341.1	10.1	16.8	41.8	−57.4	21.7	77.6	26.9	17.9	36.279	1.0191	1.010	1.009	?	N45W	I
49	9/ 8	324.1	−6.1	22.8	77.3	−76.6	37.2	53.8	13.7	39.6	23.330	1.0105	1.006	1.004	20	N55W	I
50	8/ 8	299.7	64.3	58.5	321.9	6.3	56.5	321.0	−54.8	55.0	25.761	1.0135	1.006	1.008	?	N85W	IIb
51	8/ 8	334.2	−62.2	49.7	54.2	16.2	53.4	324.6	30.5	58.3	8.708	1.0150	1.004	1.011	100	N60W	IIb
53	12/12	288.9	53.5	37.5	303.2	−38.6	53.5	24.9	1.4	47.9	21.338	1.0100	1.004	1.006	100	N50W	I
54	12/12	86.4	−11.6	38.0	0.5	11.0	39.3	305.3	−74.6	20.3	34.721	1.0472	1.037	1.010	50	N30W	III
56	11/10	58.7	−3.4	24.1	328.5	2.9	32.6	273.3	−85.5	25.5	36.442	1.0338	1.009	1.025	50	N50W	III
57	7/ 6	70.5	−1.9	10.0	340.5	5.4	33.5	318.3	−84.2	34.1	23.071	1.0171	1.012	1.005	10	N50E	IIa
58	6/ 6	292.8	−86.3	14.0	335.1	2.7	14.3	65.6	−2.6	10.6	82.884	1.0362	1.021	1.015	30	N84E	IIb
59	12/12	48.5	−13.5	33.5	322.0	42.0	56.9	317.2	−41.8	56.2	41.557	1.0134	1.006	1.006	40	N80W	III
60	12/ 8	43.2	11.4	20.4	305.5	15.8	46.5	346.2	−69.7	45.9	31.871	1.0172	1.006	1.011	100	N41E	IIa
61	12/12	357.9	−1.5	46.2	277.9	−0.6	48.0	356.0	85.0	40.5	22.592	1.0341	1.011	1.023	50	N34W	IIa
62	48/48	–	–	–	–	–	–	–	–	–	28.281	1.0216	1.012	1.010	?	N15E	IV
64	9/ 9	70.5	−6.8	25.9	319.6	−75.3	42.5	345.4	13.4	38.5	32.823	1.0200	1.008	1.012	?	N85E	I
66	12/12	–	–	–	–	–	–	–	–	–	28.658	1.0078	1.003	1.005	20	N40E	IV

Table 1 (continued)

Site	N/n	K_1			K_2			K_3			K	P	L	F	Width	Strike	Fabric
		Decl.	Incl.	Ci	Decl.	Incl.	Ci	Decl.	Incl.	Ci	(10^{-3})	K_1/K_3	K_1/K_2	K_2/K_3	(m)		type
67	12/12	83.6	16.1	52.1	8.5	−14.6	54.8	322.7	70.0	34.4	24.241	1.0167	1.008	1.008	20	N80W	IIa
68	12/ 8	355.1	4.5	35.9	85.7	−12.9	38.4	275.5	−79.8	27.0	32.010	1.0260	1.007	1.019	20	N25W	IIa
69	12/12	–	–	–	–	–	–	–	–	–	7.351	1.0176	1.011	1.006	100	N75E	IV
70	12/11	66.8	62.4	24.0	298.1	12.6	41.7	26.2	−27.7	39.8	18.101	1.0322	1.021	1.011	30	N75E	I
71	16/16	87.8	15.9	61.6	24.7	−79.7	54.4	326.5	25.7	59.2	35.279	1.0165	1.011	1.006	30	N75E	I
Curitiba																	
72	8/ 7	298.2	47.2	29.9	298.9	−46.8	37.9	30.7	2.6	35.6	34.493	1.0227	1.011	1.011	0.3	N40W	I
75	12/ 9	303.1	55.5	45.5	292.9	−34.6	46.8	26.5	−7.9	12.6	30.156	1.0245	1.006	1.018	?	N60W	I
76	8/ 8	–	–	–	–	–	–	–	–	–	26.449	1.0165	1.005	1.011	5	N-S	IV
77	12/10	318.0	−23.4	15.7	3.1	59.8	19.8	55.7	−19.9	16.2	35.031	1.0472	1.010	1.037	30	N40W	I
78	9/ 6	299.3	72.3	15.3	312.8	−17.3	15.8	41.3	3.5	5.9	44.396	1.0549	1.005	1.050	20	N60W	I
79	10/10	318.6	−15.9	46.7	65.2	−46.0	49.9	21.8	26.6	51.4	24.442	1.0311	1.012	1.019	100	N46W	I
79′	8/ 5	279.0	0.4	26.3	358.6	−78.0	18.7	8.4	10.0	23.8	28.612	1.0275	1.008	1.020	80	N71W	I
80	12/ 9	304.0	73.2	53.3	311.9	−17.1	52.8	38.3	3.0	9.9	30.652	1.0354	1.008	1.027	20	E-W	I
81	7/ 7	–	–	–	–	–	–	–	–	–	21.916	1.0115	1.006	1.006	?	N80W	IV
82	15/15	308.0	18.6	42.7	317.7	−60.8	52.2	39.8	−0.5	47.1	29.443	1.0250	1.006	1.019	10	N70W	I
85	18/14	299.3	−44.0	37.1	83.5	−45.5	35.5	14.4	18.3	37.4	30.506	1.0565	1.016	1.040	100	N76W	I
86	5/ 5	324.2	30.4	33.1	322.6	−59.5	33.6	55.4	−1.1	7.1	35.204	1.0473	1.006	1.041	80	N70W	I
87	5/ 5	289.9	62.8	21.5	302.2	−26.1	23.1	30.2	4.5	13.2	17.393	1.0609	1.007	1.054	30	N56W	I
92	4/ 4	348.2	62.6	48.8	300.1	−27.4	51.6	63.6	−26.5	38.3	0.867	1.0034	1.001	1.002	40	N30W	I
93	7/ 7	19.5	−69.4	33.7	318.3	21.3	60.6	21.3	11.6	58.1	24.520	1.0211	1.010	1.011	20	N44E	IIb
94	7/ 7	7.2	−77.0	29.4	308.6	7.0	25.3	36.6	11.9	20.5	28.462	1.0527	1.020	1.032	?	N65W	I
95	11/10	58.4	23.4	32.2	328.4	0.5	32.5	61.1	−65.5	13.1	39.590	1.0284	1.006	1.022	120	N74E	IIa
96	15/15	293.0	−31.9	49.3	307.5	57.8	48.7	29.9	−3.6	31.9	31.718	1.0312	1.008	1.023	?	N66W	I
98	4/ 4	308.2	−27.2	43.2	73.6	−40.6	42.7	11.2	25.4	35.4	41.879	1.0280	1.007	1.020	?	N56W	I
99	12/12	356.8	43.7	40.4	302.1	−31.1	43.5	49.0	−28.1	16.9	33.750	1.0703	1.013	1.057	40	N30W	I
100	4/ 3	352.6	−83.1	12.7	298.1	4.0	13.6	28.7	5.2	6.1	40.830	1.0951	1.006	1.089	20	N30W	I
101	10/ 7	274.0	11.3	35.7	320.7	−66.7	35.2	7.5	22.0	29.7	23.284	1.0300	1.007	1.022	60	N60W	I
102	6/ 5	289.9	−47.7	34.1	309.0	40.6	35.4	31.8	−9.9	13.3	29.440	1.0318	1.008	1.024	70	N41W	I
103	3/ 3	284.8	−28.9	18.7	312.6	57.8	26.4	19.5	−14.1	18.8	27.114	1.0158	1.006	1.009	60	N71W	I
104	36/36	300.9	69.1	33.9	291.2	−26.8	49.5	23.9	−5.5	47.3	34.798	1.0358	1.017	1.019	150	N60W	I
122	12/12	43.9	−3.6	9.6	312.1	13.1	38.5	295.9	−76.1	39.1	31.999	1.0510	1.041	1.009	4	N30E	IIa
123	8/ 8	38.8	4.4	36.1	298.3	−45.5	51.9	297.8	49.3	43.7	15.624	1.0335	1.026	1.007	10	N30E	IIa
Guapiara																	
105	16/16	292.3	−66.7	57.8	284.7	10.5	61.1	16.1	8.4	29.8	27.464	1.0129	1.004	1.009	50	N67W	I
106	9/ 6	323.9	−29.9	19.5	46.1	16.0	24.4	293.5	56.1	22.1	91.067	1.0217	1.009	1.013	?	N60W	IIa
107	11/11	311.4	24.2	40.7	334.1	−61.2	39.1	48.2	10.8	20.6	25.348	1.0386	1.006	1.032	200	N32W	I
113	12/ 9	25.1	−17.0	15.9	299.9	14.3	19.4	68.6	68.0	13.3	33.563	1.0153	1.008	1.007	30	N40W	III
114	12/ 9	293.4	−19.0	31.2	348.5	58.8	35.1	33.0	−24.7	20.4	38.064	1.0170	1.004	1.012	100	N47W	I
115	8/ 8	13.9	21.8	45.8	52.3	−62.4	47.9	298.9	−11.9	29.1	30.360	1.0144	1.011	1.003	3	N10E	I
116	8/ 8	49.3	12.4	24.9	346.2	−69.8	35.8	318.9	15.8	32.3	0.696	1.0086	1.007	1.002	?	N50E	I
118	12/12	0.3	17.3	43.5	294.4	−57.0	39.6	84.6	−39.8	53.2	50.631	1.0405	1.033	1.007	10	N20W	I
131	10/10	277.5	−9.6	31.8	324.8	77.0	45.5	13.3	−4.7	42.9	63.636	1.0230	1.010	1.013	?	N35W	I
132	13/13	79.3	−7.3	30.7	344.6	−15.9	30.6	24.8	72.1	23.9	44.611	1.0151	1.007	1.009	?	N78E	IIa
133	8/ 8	318.2	7.3	28.4	85.1	78.5	21.1	47.4	−5.5	21.6	26.538	1.0242	1.010	1.014	?	N7W	I
134	4/ 4	46.1	52.2	23.8	285.4	21.6	46.2	9.2	−24.6	45.8	74.849	1.0192	1.013	1.006	?	N63E	I
135	10/10	318.9	42.8	50.4	336.6	−51.6	53.2	51.2	9.2	22.4	32.673	1.0207	1.004	1.017	?	N40W	I

N, number of specimens per site; n, number of specimens included in the AMS means; K_1, K_2, K_3, maximum, intermediate and minimum susceptibility intensities; Decl, Incl, declination and inclination for the mean susceptibility axes; Ci, angular dispersion; K, mean susceptibility; P, mean anisotropy degree; L, lineation; F, foliation. All susceptibility values are given in SI units.

processes. Comprehensive reviews have been given by Hrouda (1982), MacDonald and Ellwood (1987), Jackson and Tauxe (1991), Rochette et al. (1992) and Tarling and Hrouda (1993). The characterization of igneous fabric by means of AMS has been useful for determining the primary igneous flow (e.g. Khan, 1962; Ellwood, 1978), thermal contraction owing to cooling (e.g. Ellwood, 1979) or deformation following emplacement (e.g. Ellwood, 1978). Regarding dykes, AMS has been applied for studying tectonic problems (Park et al., 1988) and magma flow direction during the filling of fractures (e.g. Knight and Walker, 1988; Ernst, 1990; Ernst and Baragar, 1992; Staudigel et al., 1992). In this paper, the AMS technique is applied to determine the magnetic fabric of the Ponta Grossa (PG) dykes and to investigate the mode of magma flow injection.

2. The Ponta Grossa dyke swarm

One of the largest Phanerozoic mafic dyke swarms in Brazil occurs in the Ponta Grossa Arch (Sial et al., 1987), a tectonic feature on the eastern border of the Palaeozoic–Mesozoic Paraná Basin (Fig. 1). This Arch occupies about 134 000 km^2 in area. According to Almeida (1986), the area was most active during the Jurassic and Lower Cretaceous, when its structures were enhanced and the Arch took its present configuration. The dykes as well as the volcanic rocks of the Paraná Basin are related to the break-up of Gondwanaland, having been emplaced during rifting before the outpouring of mid-ocean ridge basalts that formed the initial Atlantic Ocean crust (Almeida, 1986; Piccirillo et al., 1988). Radiometric Ar–Ar ages for some PG dykes vary from 133.9 ± 2.5 to 130.4 ± 2.9 Ma (Turner et al., 1994), and are similar to those for the Paraná Basin volcanics based on the same method (Renne et al., 1992; Turner et al., 1994). However, palaeomagnetic data (Raposo and Ernesto, 1989; Raposo, 1992) reveal that the dykes are actually younger than the major part of the volcanic rocks in the basin. This is reinforced by the fact that some dykes, although rare, can be seen cutting acid and basic flows, mainly in the northern part of the Paraná basin (Fartura region, Fig. 1).

The dykes are concentrated in the regions of Sapopema, Telêmaco Borba and Fartura, where they intrude the Palaeozoic sedimentary rocks of the Paraná Basin, and in the regions of Curitiba and Guapiara, where they intrude the Precambrian rocks of the crystalline basement (Fig. 1). According to Benini (1992) and Piccirillo et al. (1990), they are formed by andesi-basalt tholeiites and rare acid rocks (De La Roche et al. (1980) classification); thicknesses vary from tens to hundreds of metres and the dykes may be tens of kilometres in length. They are fine to medium grained, and no difference in grain size is evident for dykes cutting Palaeozoic or Precambrian terrains. The most coarse-grained diabase was found intruding sediments in the western part of the Arch, near Sapopema (Fig. 1). The PG dykes trend mainly NW and dip vertically or near vertically. During sampling, both NW and NE strikes (Table 1) were measured.

3. Anisotropy of magnetic susceptibility

The AMS of rocks provides a measure of the preferred orientation of magnetic minerals. This type of anisotropy corresponds to the magnetic susceptibility (K) variation with the measured sample axes or the direction of the applied field. The AMS corresponds to a tensor of the second rank which can be represented by an ellipsoid with principal axes K_1 (maximum susceptibility), K_2 (intermediate susceptibility) and K_3 (minimum susceptibility). The directions of the susceptibility axes are described by declination and inclination angles.

The AMS of a rock can be caused by several factors, as reported, for example, by Stacey (1960), Uyeda et al. (1963), Hrouda (1982) and Hargraves et al. (1991). In rocks where the main magnetic minerals are titanomagnetites the AMS is controlled by the shape of the grains (non-sphericity of individual grains). Shape anisotropy, owing to aligned elongated particles or planar/linear distribution of particles, seems to be the most common cause of AMS in basaltic rocks such as those in this study.

The discussion on whether the principal AMS ellipsoid axes are related to the motion of magmatic laminar flow has been the subject of many investigations, mostly based on experimental data. For example, Khan (1962), using both the AMS technique and microscope analyses, showed that the physical orientation of magnetite—long, intermediate and short grain axes—corresponds very closely to the principal AMS ellipsoid axes, as Graham (1954) had already reported. Rees (1968, 1979) suggested that elongated grains may align parallel to the flow direction. Knight and Walker (1988), by comparing the magnetic fabric with the macroscopic surface lineations in dykes of the Koolau Complex, concluded that the K_1 axes parallel the attitudes of macroscopic flow lineations. Therefore clusters of K_1 axes may represent the flow azimuths or the absolute magma flow directions in dyke swarms. On the other hand, Ellwood (1978) occasionally found intermediate axes (K_2) paralleling the flow lines.

4. AMS measurements

The AMS measurements were performed in samples from 95 dykes for which azimuths could be determined. Samples were originally collected for palaeomagnetic analysis. Most of the samples are hand-blocks but also some cylinders were taken with the aid of a gasoline-powered rock drill. Sample orientation was performed by both magnetic and sun compasses, whenever possible. Normally three samples (or 6–9 cylinders) were collected from each dyke distributed through the exposed width. In the favourable outcrops a more detailed sampling was performed, including both margins as well as the centre. For the analytical work, samples were cut into cylindrical specimens 2.5 cm in diameter and 2.2 cm in height. A total of 989 specimens were measured in a Minisep instrument (Molspin, Newcastle upon Tyne, UK). As the AMS measurements were performed after the palaeomagnetic work, a large number of specimens were previously submitted to a.f. cleaning in a tumbling Molspin instrument. In these cases,

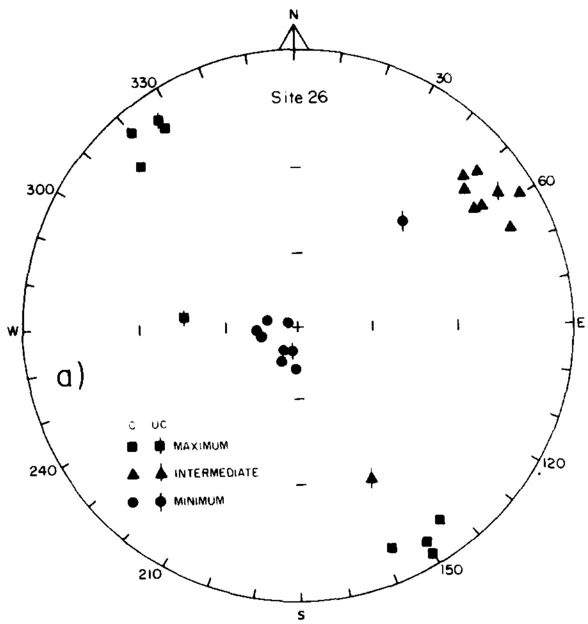

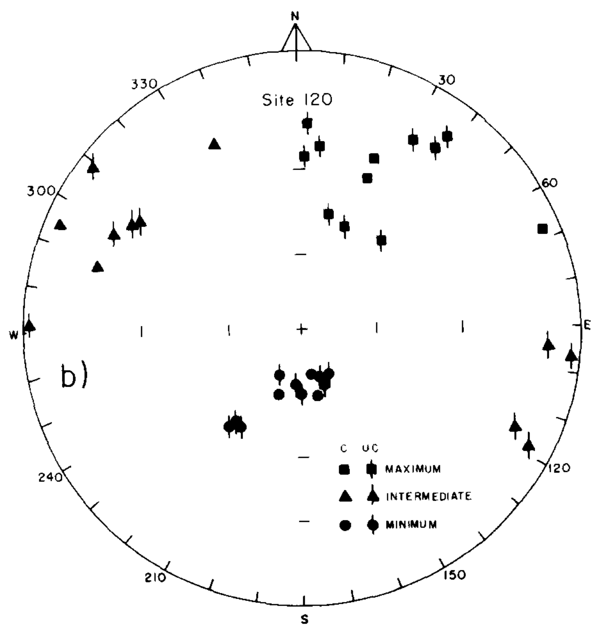

Fig. 2. AMS results for specimens from Sites 26 and 120 located in Sapopema and Fartura regions, respectively. The three axes are represented for uncleaned (UC) and a.f. cleaned (C) specimens in a tumbling (a) and static (b) demagnetizer. Plot in lower hemisphere.

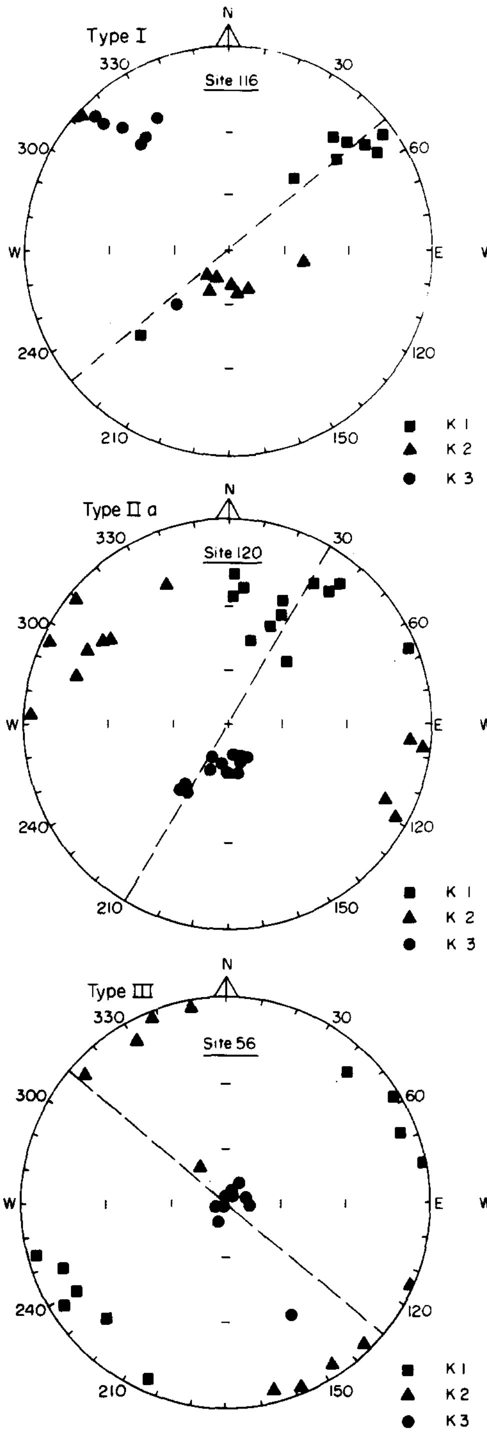

Fig. 3. Examples of the fabric types found in the Ponta Grossa dykes. Magnetic anisotropy data (maximum, intermediate and minimum susceptibility axes are respectively squares, triangles and circles) plotted in lower hemisphere. Dashed line represents the dyke plane assuming vertical dip.

the pilot-specimen of each sample underwent fields up to 80 mT whereas the companion specimens were demagnetized in fields normally not greater than 35 mT. However, for all sites (dykes) at least one untreated specimen was measured. In general, results for cleaned samples clustered better than those for the uncleaned ones, as can be seen in the example of Fig. 2(a). This effect is particularly true for samples with higher initial magnetic remanence, and can be related to the existence of a domain anisotropy superimposed on the shape anisotropy, as suggested by Park et al. (1988). This behaviour was also noticed by Rochette et al. (1992) for some samples with weak anisotropy.

A static a.f. demagnetizer (Sapphire Instruments, Ruthven, Ont., Canada) was also used to clean the pilot-specimens of Sites 107, 115, 116, 118 and 120 before the AMS measurements. For each demagnetization step the specimen was submitted to the same peak field according to three orthogonal axes (x, y and z). The AMS of all other specimens refers to uncleaned samples. Although it has been already suggested by Potter and Stephenson (1990a,b) that the static demagnetization could impart an spurious AMS, these results were not discarded as they are few in number compared with the total number of analysed specimens in each site, as seen for Site 120 in Fig. 2(b). Furthermore, these results did not give clear evidence for such effects in the PG samples.

Measurements also provided the mean susceptibility or bulk susceptibility, expressed as $K = (K_1 + K_2 + K_3)/3$ in SI units, as well as the anisotropy parameters given by the ratios $P = K_1/K_3$, $L = K_1/K_2$ and $F = K_2/K_3$ corresponding to the anisotropy degree, lineation and foliation, respectively (Table 1). The mean susceptibility is generally high, as normally found in basaltic rocks, whereas the anisotropy degree is low, with P varying between 1.0034 and 1.0951 (average of 1.0258).

The mean directions for axial data were calculated using principal component analysis and the confidence angle Ci (Table 1) given by Schmidt et al. (1988). This statistical parameter is defined as $Ci = \cos^{-1}(Si)$, where $Si = \lambda_i/(\lambda_1 + \lambda_2 + \lambda_3)$ and λ_1, λ_2 and λ_3 are the eigenvalues of the mean AMS ellipsoid. This parameter gives an estimate of the angular dispersion for the AMS axial clusters similarly to Fisher's (1953) α_{95} confidence circle, used in Fisherian statistics for palaeomagnetic data. However, Ci is less strongly dependent upon the number of observations. This allows one to compare directly angular dispersion between data sets with varying number of samples (as is the case in this paper). More rigorous statistical methods have been given by Jelinek (1978) and Constable and Tauxe (1990). However, these methods require a large number of observations per site, as discussed by Lienert (1991). As stated by Schmidt et al. (1988), Ci was designed to overcome difficulties encountered in more rigorous statistical methods of AMS data evaluation where a larger number of observations per site are required. Within individual dykes, AMS directions are usually well grouped. However, some scattered results were rejected (Table 1). Only seven dykes showed no clear clustering and therefore their means are not reported in Table 1.

5. Magnetic fabric

The analysis at the single dyke scale defines four main fabric types according to the orientation of the mean magnetic axes with respect to the dyke plane. These fabric types, coded I–IV, are described below, and examples are shown in Fig. 3.

Fabric Type I is characterized by the clustering of K_1 and K_2 axes on the dyke plane, whereas K_3 axes are nearly perpendicular to the dyke plane (the mean K_3 inclinations depart less than 30° from the horizontal plane). This fabric type corresponds to 51% (Fig. 4) of the PG dykes.

Fabric Type II is defined by K_1 and K_3 axes clustering close to the dyke plane. This type characterizes 38% of the PG dykes (Fig. 4), and still can be subdivided into two categories. In one of them (Type IIa, Fig. 3), K_3 is nearly vertical and the mean K_1 inclinations normally do not exceed 25°. The second category (Type IIb, Fig. 3) is represented by only seven dykes with K_1 inclina-

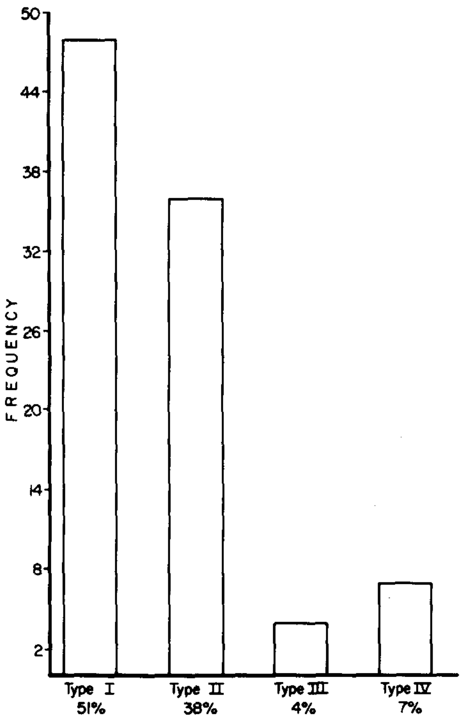

Fig. 4. Frequency diagram of the fabric types in PG dykes.

tions greater than 40° and K_3 inclinations varying from approximately horizontal ($I_3 < 15°$) to inclined ($30° < I_3 < 54°$).

In Type III fabric, however, K_2 and K_3 are the axes forming a plane nearly parallel (within ±25°) to the dyke plane and K_1 is perpendicular to that plane (mean K_1 inclination approximately 15°). This type was recognized in only four of the PG dykes (Fig. 4).

In Type IV fabric, the AMS axes did not show clearly a preferred orientation or were randomly oriented. This fabric type occurred in the remaining 7% of the dykes. In these cases, mean directions are not meaningful and were not included in Table 1.

The plot of L vs. F parameters (Fig. 5) expressed as mean values for each dyke shows that the magnetic fabric shape tends to be more foliated than lineated. However, large F values are mostly observed for Type I fabric. Fabric Types I and II are present in all studied regions, as can be seen in Fig. 6. However, in the Curitiba and Guapiara regions, Type I is more frequent than in other regions.

6. Origin of the fabric types

The magnetic minerals in the PG dykes are mainly phenocrysts and groundmass crystals of titanomagnetite highly oxidized at high temperatures (i.e. textural scheme of Haggarty (1981)). This oxidation state is indicated by the Curie temperatures in the range 500–580°C observed in the thermomagnetic curves (Fig. 7), and by the phenocrysts and microphenocrysts of ilmenite as observed on polished sections. The titanomag-

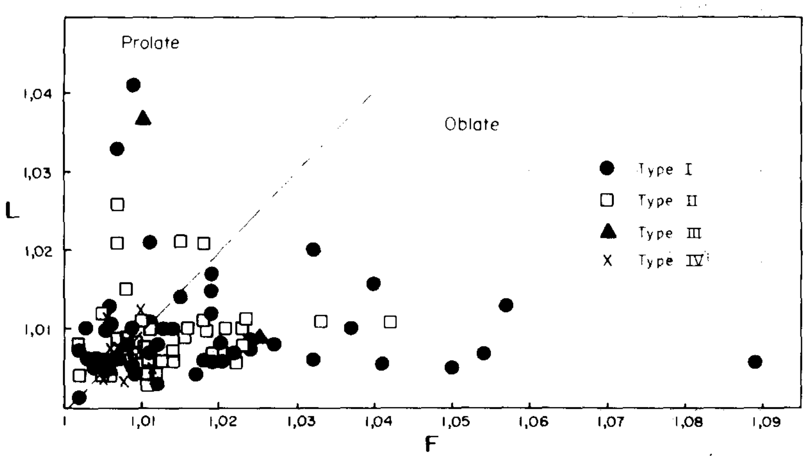

Fig. 5. Dyke mean values for the anisotropy ratios L vs. F for all fabric types.

netites were crystallized at 1176°C, according to Piccirillo et al. (1990), and no evidence of later alterations by hydrothermalism or metamorphism

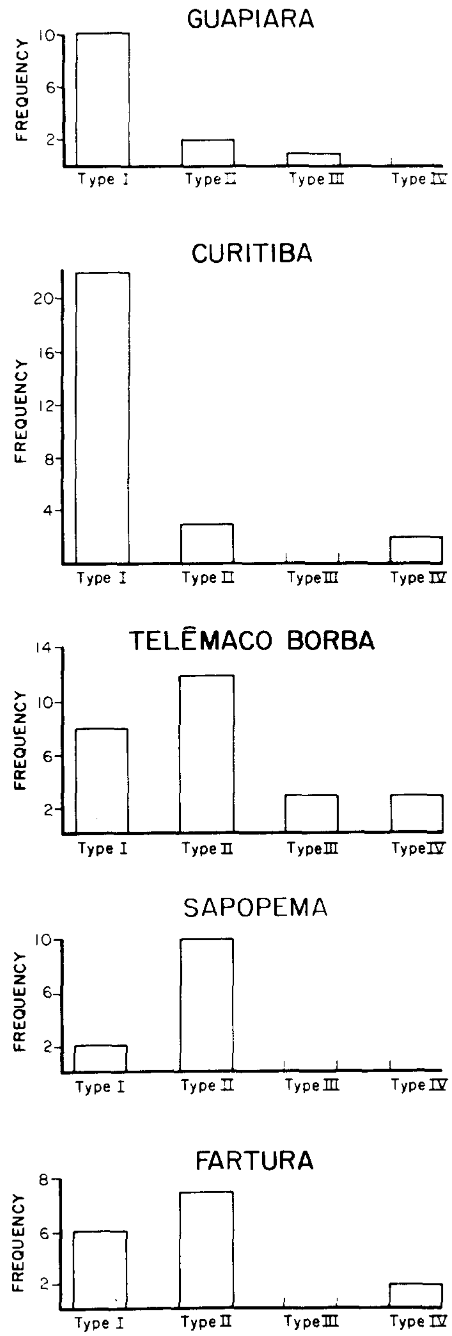

Fig. 6. Frequency diagram for the fabric types in the Fartura, Sapopema, Telêmaco Borba, Guapiara and Curitiba regions.

exists in the magnetic minerals or the silicates (plagioclases and pyroxenes). The magnetic characteristics of the PG samples identified during palaeomagnetic analysis (Raposo, 1992) suggest a multidomain grain state as indicated by median destructive fields generally in the range 10–30 mT. For this reason, the possibility of the long grain axes becoming the minimum susceptibility axes, as is commonly observed when single-domain grains are the AMS carriers (Potter and Stephenson, 1988), is discounted. The above arguments indicate that all the magnetic fabric types recognized in the Ponta Grossa dykes are probably of primary origin.

Fabric Type I is in agreement with the fabric type reported by Rochette et al. (1991) for basaltic dykes from the Oman ophiolite and referred to as 'normal magnetic fabric' reflecting magma flow. In this case, the K_1 axis is parallel to the flow line and the K_3 axis is perpendicular to the dyke walls, as already shown by many workers (Ellwood, 1988; Knight and Walker, 1988; Ernst and Baragar, 1992; Rochette et al., 1992; Staudigel et al., 1992). Fabric Type II is similar to that found by Park et al. (1988) in the Proterozoic Mealy dyke swarm of Labrador. They attributed this fabric to a vertical compaction of a static magma column with the minimum stress along the dyke direction. Fabric Type II may be similarly explained by these dykes having acted as stress conduits, with continuing compression tending to force material along strike. Fabric Type III was found in only four dykes. This fabric is abnormal and similar to the inverse or reverse magnetic fabric found for the Oman dykes (Rochette et al., 1991). In this case, the magnetic fabric was attributed to secondary processes such as hydrothermalism which, however, do not apply to PG dykes. Ellwood (1978), when studying Icelandic dykes, suggested that statistically significant clustering of the K_2 axis in the nearly vertical K_1 and K_2 or K_2 and K_3 planes may indicate the dyke emplacement direction. However, all magnetic fabric Type III dykes do not show the same significant K_2 cluster and K_3 are vertically directed. Hargraves et al. (1991) found K_1 perpendicular to the dyke plane in samples near the margins for Brazilian Precambrian dykes. This was interpreted as the result of the growth of mineral inward from the cooling surface. In the PG dykes, however, samples from both margin and centre of the bodies show the K_1 axis perpendicular to the dyke plane, characterizing a different situation which probably cannot be similarly explained.

7. Magma flow in the Ponta Grossa dykes

The possible origins for the different fabric types recognized in the PG dykes were discussed earlier. It was concluded that fabric Type I better reflects magma flow during dyke emplacement, and this assumption will be made to investigate the mode of emplacement of the PG dykes. The K_1 inclinations (Fig. 8) in the majority of the dykes (58%) were fed by horizontal or sub-horizontal ($I_1 < 30°$) magma fluxes, and 42% were fed by inclined to vertical fluxes. The K_1 inclinations

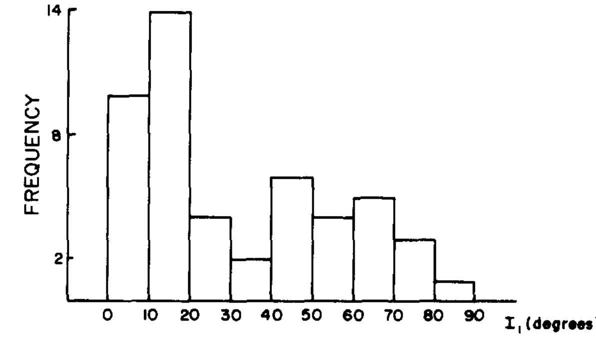

Fig. 8. Frequency diagram of the K_1 inclination for fabric Type I.

are steepest in the Curitiba region (Fig. 9). This suggests that this area could have been closer to a magma source, as steeper flow planes may indicate the proximity of the source, as reported for example by Ernst (1990). However, it is not plausible to predict only one magma source acting inside the Ponta Grossa arch because contempo-

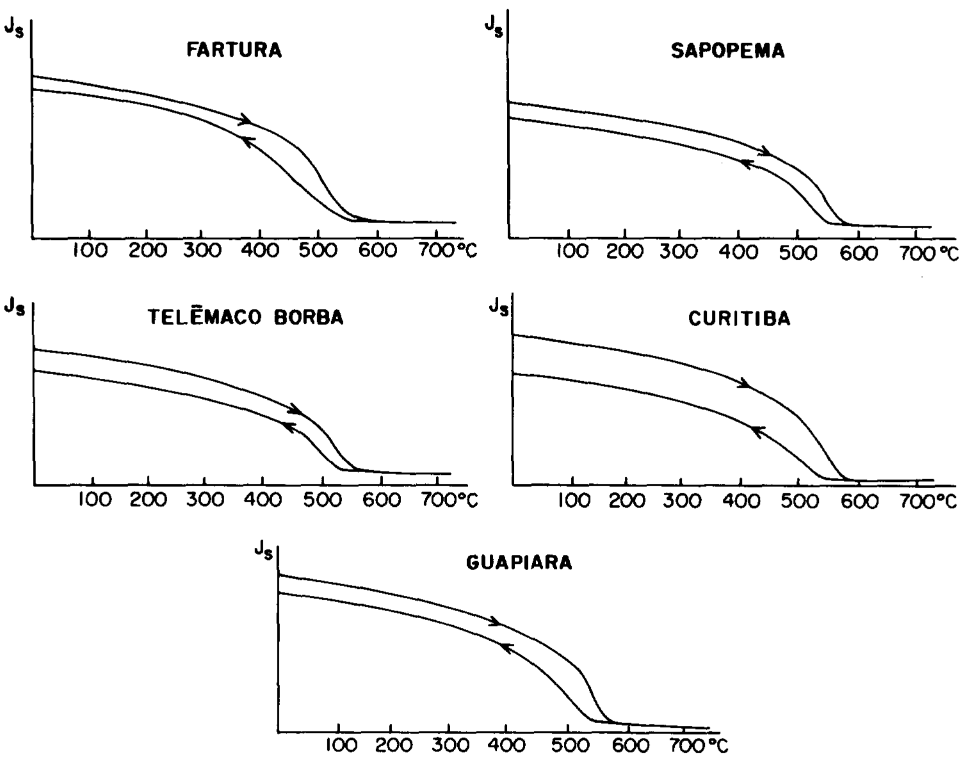

Fig. 7. Representative thermomagnetic curves for samples of the Ponta Grossa dykes. Heating rate of 50°C min^{-1}; magnetic fields of 0.4 T; Js is saturation magnetization in arbitrary units.

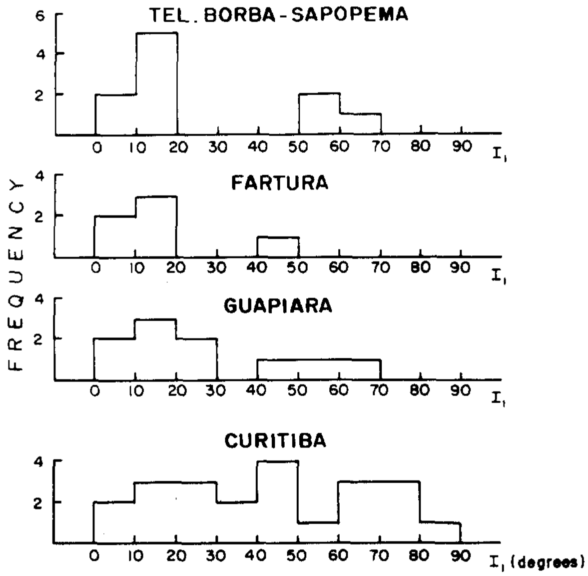

Fig. 9. Variation of the K_1 inclination (fabric Type I) in the Ponta Grossa Arch region.

raneous dykes were fed by compositionally distinct magmas (Piccirillo et al., 1990; Benini, 1992), as indicated by palaeomagnetic data (Raposo, 1992). The most remarkable chemical difference is between most primitive Curitiba and the most evolved rock Fartura dykes. Fartura and Guapiara are the best correlatable areas from both a chemical and a palaeomagnetic point of view, suggesting a contemporaneous magmatic activity. However, the magma flow in the Guapiara dykes tends to be more inclined than in the Fartura dykes (Fig. 9), which may indicate that one possible source would be closer to Guapiara. On the other hand, the vertical distances from the magma source to the crustal levels at which the dykes are observed nowadays seem shorter in Guapiara (Precambrian area) than in Fartura, where the dykes may cut even the Lower Cretaceous lava flows. Horizontal magma flow means lateral magma injection inside fractures, and becomes more probable as the source is located further away (Ernst, 1990). In this case, it is also reasonable to expect a more evolved magma. Curitiba and Sapopema–Telêmaco Borba dykes show some different characteristics in their chemical composition, but here again the dykes which are seen in Palaeozoic levels (Sapopema–Telêmaco Borba) were fed preferentially by lateral injections, whereas in the Precambrian terrains (Curitiba) the flows are steeper. However, some dykes showing inclined flow are also found in Sapopema–Telêmaco Borba, suggesting possible independent sources in this region.

8. Conclusions

From the AMS data for the Ponta Grossa dyke swarm, the following conclusions can be drawn:

(1) four types of magnetic fabric which are of primary origin (Types I–IV) can be recognized. Types I and II are the most important and correspond to 89% of the investigated dykes.

(2) Fabric Type I is characterized by the clustering of K_1 and K_2 axes on the dyke plane, whereas K_3 axes are nearly perpendicular to the dyke plane. This fabric type is the only one associated with magma flow.

(3) Fabric Type II is defined by K_1 and K_3 axes clustering close to the dyke plane, and K_2 axes are perpendicular to that plane. This type is interpreted as resulting from magma under stress. It is particularly important in those dykes emplaced in sediments (Fartura, Sapopema and Telêmaco Borba regions).

(4) The majority of the PG dykes (58%) were fed laterally, i.e. by a horizontal magma flow.

(5) In the Curitiba area the magma flow planes are on average steeper than in other regions, suggesting the proximity of a magma source in this area.

Acknowledgements

The authors wish to thank R. Ernst for the valuable suggestions and comments. B.B. Ellwood made a very helpful review of an earlier version of the manuscript. This paper was substantially improved by two anonymous referees. One of the authors (M.E.) is indebted to Dr. N. Petersen of the University of Munich for introducing her to AMS studies during her visit to his laboratory. Financial support was given by the Brazilian agencies FAPESP and FINEP.

References

Almeida, F.F.M., 1986. Distribuição regional e relações tectônicas do magmatismo pós-Paleozóico no Brasil. Rev. Bras. Geocienc., 16: 325–349.

Baer, G. and Reches, Z., 1987. Flow patterns of magma in dikes, Makhtesh Romon, Israel. Geology, 15: 569–572.

Benini, S., 1992. Sciami di dicchi nel S-E Brasile: petrologia, geochimica isotopica e implicazioni geodinamiche. Ph.D. Thesis, University of Trieste, 123 pp.

Constable, C. and Tauxe, L., 1990. The bootstrap for magnetic susceptibility tensors. J. Geophys. Res., 95(B6): 8383–8395.

Coward, M.P., 1980. The analysis of flow profiles in a basaltic dyke using strained vesicles. J. Geol., 137: 605–615.

De La Roche, H., Leterrier, P., Grandclaud, P. and Marchal, M., 1980. A classification of volcanic and plutonic rocks using R_1-R_2 diagram and major element analyses. Its relationship with current nomenclature. Chem. Geol., 29: 183–210.

Ellwood, B.B., 1978. Flow and emplacement direction determined for selected basaltic bodies using magnetic susceptibility anisotropy measurements. Earth Planet. Sci. Lett., 41: 254–264.

Ellwood, B.B., 1979. Anisotropy of magnetic susceptibility variations in Icelandic columnar basalts. Earth Planet. Sci. Lett., 42: 209–212.

Ellwood, B.B., 1988. Anisotropy of magnetic susceptibility: empirical evaluation of instrumental precision. Geophys. Res. Lett., 11: 645–648.

Ernst, R.E., 1990. Magma flow directions in two mafic Proterozoic dyke swarms of the Canadian shield, as estimated using anisotropy of magnetic susceptibility data. In: A.J. Parker, P.C. Rickwood and D.H. Tucker (Editors), Mafic Dykes and Emplacement Mechanisms. Balkema, Rotterdam, pp. 231–235.

Ernst, R.E. and Baragar, W.R.A., 1992. Evidence from magnetic fabric to the flow pattern of magma in the Mackenzie giant radiating dyke swarm. Nature, 356: 511–513.

Fisher, R.A., 1953. Dispersion on a sphere. Proc. R. Soc. London, Ser. A, 217: 295–305.

Graham, J.W., 1954. Magnetic susceptibility anisotropy, an unexploited petrofabric element. Geol. Soc. Am. Bull., 75: 1257–1258.

Greenough, J.D., Ruffman, A. and Owen, J.V., 1988. Magma injection directions inferred from fabric study of the Popes Harbour dike, eastern shore, Nova Scotia, Canada. Geology, 16: 547–550.

Haggarty, S.E., 1981. Oxidation of opaque mineral oxides in basalts. In: D. Rumble (Editor), Reviews in Mineralogy (Vol. 3), Oxides Minerals: Chapter 4, Mineralogical Society of America, Washington, DC.

Hargraves, D., Johnson, D. and Chan, C.Y., 1991. Distribution anisotropy: the cause of AMS in igneous rocks? Geophys. Res. Lett., 18: 2193–2196.

Hrouda, F., 1982. Magnetic anisotropy of rocks and its applications in geology and geophysics. Geophys. Surv., 5: 37–82.

Jackson, M. and Tauxe, L., 1991. Anisotropy of magnetic susceptibility and remanence: developments in the characterization of tectonic, sedimentary and igneous fabric. Rev. Geophys., Suppl.: 371–376.

Jelinek, V., 1978. Statistical processing of anisotropy of magnetic susceptibility measured on groups of specimens. Studia Geophys. Geod., 22: 50–63.

Khan, M.A., 1962. The anisotropy of magnetic susceptibility of some igneous and metamorphic rocks. J. Geophys. Res., 67: 2873–2885.

Knight, M.D. and Walker, G.P.L., 1988. Magma flow directions in dikes of the Koolau Complex, Oahu, determined from magnetic fabric studies. J. Geophys. Res., 93(B5): 4301–4319.

Komar, P.D., 1972. Mechanical interactions of phenocrysts and flow differentiation of igneous dykes and sills. Geol. Soc. Am. Bull., 83: 973–988.

Lienert, B.R., 1991. Monte Carlo simulation of errors in the anisotropy of magnetic susceptibility: a second-rank symmetric tensor. J. Geophys. Res., 96(B12): 19539–19544.

MacDonald, W.D. and Ellwood, B.B., 1987. Anisotropy of magnetic susceptibility: sedimentological, igneous, and structural–tectonic applications. Rev. Geophys., 25: 905–909.

Park, K., Tanczyk, E.I. and Desbarats, A., 1988. Magma fabric and its significance in the 1400 Ma Mealy diabase dykes of Labrador, Canada. J. Geophys. Res., 93(B11): 13689–13704.

Piccirillo, E.M., Melfi, A.J., Comin-Chiaramonti, P., Bellieni, G., Ernesto, M., Marques, L.S., Nardy, A.J.R., Pacca, I.G., Roisemberg, A. and Stolfa, D., 1988. Continental flood volcanism from the Paraná Basin (Brazil). In: J.D. MacDougal (Editor), Continental Flood Basalts. Kluwer Academic, Dordrecht, pp. 195–238.

Piccirillo, E.M., Bellieni, G., Cavazzini, G., Comin-Chiaramonti, P., Petrini, R., Melfi, A.J., Pinese, J.P.P., Zantedeschi and De Min, A., 1990. Lower Cretaceous tholeiitic dyke swarm from the Ponta Grossa Arch (Southeast Brazil): petrology, Sr–Nd isotopes and genetic relationships with the Paraná flood volcanics. Chem. Geol., 89: 19–48.

Potter, D.K. and Stephenson, A., 1988. Single-domain particles in rocks and magnetic fabric analysis. Geophys. Res. Lett., 15: 1097–1100.

Potter, D.K. and Stephenson, A., 1990a. Field-impressed anisotropies of magnetic susceptibility and remanence in minerals. J. Geophys. Res., 95(B10): 15573–15588.

Potter, D.K. and Stephenson, A., 1990b. Field-impressed magnetic anisotropy in rocks. Geophys. Res. Lett., 17: 2437–2440.

Raposo, M.I.B., 1992. Paleomagnetismo do enxame de diques do Arco de Ponta Grossa. Ph.D. Thesis, University of São Paulo, 105 pp.

Raposo, M.I.B. and Ernesto, M., 1989. Rochas intrusivas básicas do Arco de Ponta Grossa: resultados paleomagnéticos preliminares. Rev. Bras. Geocienc., 19: 393–400.

Rees, A.I., 1968. The production of preferred orientation in a concentrated dispersion of elongated and flattened grains. J. Geol., 76: 457–465.

Rees, A.I., 1979. The orientation of grains in sheared dispersion. Tectonophysics, 55: 275–287.

Renne, P.R., Ernesto, M., Pacca, I.G., Coe, R.S., Glen, J.M., Prevot, M. and Perrin, M., 1992. The age of Parana flood volcanism, rifting of Gondwanaland, and Jurassic–Cretaceous boundary. Science, 258: 975–979.

Rochette, P., Jenatton, L., Dupy, C., Boudier, F. and Reuber, I., 1991. Emplacement mode of basaltic dikes in the Oman Ophiolite: evidence from magnetic anisotropy with reference to geochemical studies. In: T.J. Peten, A. Nicolas and R. Coleman (Editors), Ophiolite Genesis and the Evolution of the Oceanic Lithosphere. Kluwer Academic, Dordrecht, pp. 55–82.

Rochette, P., Jackson, M. and Aubourg, C., 1992. Rock magnetism and the interpretation of anisotropy of magnetic susceptibility. Rev. Geophys., 30: 209–226.

Ross, M.E., 1986. Flow differentiation, phenocryst alignment, and compositional trends within a dolerite dike at Rockport, Massachusetts. Geol. Soc. Am. Bull., 97: 232–240.

Schmidt, V.A., Ellwood, B.B., Nagata, T. and Noltimier, H.C., 1988. The measurement of anisotropy of magnetic susceptibility using a cryogenic (Squid) magnetometer and a comparison with results obtained from a torsion-fiber magnetometer. Phys. Earth Planet. Inter., 51: 365–378.

Shelley, D., 1985. Determining paleo-flow directions from groundmass fabrics in the Lyttelton radial dykes, New Zealand. J. Volcanol. Geotherm. Res., 25: 69–79.

Sial, A.N., Oliveira, E.P. and Choudhuri, A., 1987. Mafic dyke swarms of Brazil. Geol. Assoc. Can. Spec. Pap., 34: 467–481.

Stacey, F.D., 1960. Magnetic anisotropy of igneous rocks. J. Geophys. Res., 65: 2429–2442.

Staudigel, H., Gee, J., Tauxe, L. and Varga, R.J., 1992. Shallow intrusive directions of sheeted dikes in the Troodos ophiolites: anisotropy of magnetic susceptibility and structural data. Geology, 20: 841–844.

Tarling, D.H. and Hrouda, F. (Editors), 1993. The Magnetic Anisotropy of Rocks. Chapman and Hall, London.

Turner, S., Regelous, M., Kelley, S., Hawkesworth, C. and Mantovani, M.S.M., 1994. Magmatism and continental break-up in the South Atlantic: high precision $^{40}Ar-^{39}Ar$ geochronology. Earth Planet. Sci. Lett., 121: 333–348.

Uyeda, S., Fuller, M.D., Belshé, J.C. and Girdler, R.W., 1963. Anisotropy of magnetic susceptibility of rocks and minerals. J. Geophys. Res., 68: 279–291.